Raman scattering study of phase transitions in $Cs_{1-x}(NH_4)_xH_2AsO_4$ mixed crystals

Chang Ju Kim and Jong-Jean Kim*
Physics Department and Center for Molecular Science, Korea Advanced Institute of Science and Technology, Taejon 305-701, Korea
(Received 28 October 1998)

Temperature dependence of Raman scattering spectra in the cesium-ammonium dihydrogen arsenate (CADA-x, $x=0.20$) mixed crystal was observed to study anomalies associated with the dipole glass freezing phenomena in the system. A_1 symmetry internal vibrations of arsenate ions were found to deviate from the normal temperature dependence of the third and fourth order anharmonic phonon-phonon interactions at around $T_f \simeq 80$ K, which was ascribed to the onset of the short range random potential fixing of protons. The B_2 symmetry soft mode derived from the harmonic oscillator coupled mode analysis was found to be a relaxational type characterized by $\omega^2/\gamma \propto (T-T_o)$ with $T_o \simeq 28.8$ K, where ω^2/γ corresponds to the relaxation bandwidth of the soft mode. The large difference between the two anomaly temperatures was attributed to the enhanced effective piezoelectric constant associated with the electrostrictive contributions from the random local cluster polarizations. [S0163-1829(99)01217-5]

I. INTRODUCTION

Mixed crystals between ferroelectric and antiferroelectric potassium dihydrogen phosphate (KDP) family crystals in a certain range of mixing concentration are known to exhibit a glass transition to a low-temperature phase of dipole glass.[1–3]

In the dipole glass forming systems the quenched random site distribution of NH_4^+ ions leads to the randomly competing interaction bonds between the proton pseudospins of the O-H$\cdots$O hydrogen bonding network. Furthermore, random substitution of NH_4^+ ions in place of Rb^+ ions also brings about extra hydrogen bonding with one oxygen of the O-H$\cdots$O bond nearby to the NH^+ ion, which fixes the pseudospin configuration of O-H$\cdots$O clusters as a random bias field for either ferroelectric or antiferroelectric local polarizations.

The random bias field due to a strong electrostatic coupling between the O-H$\cdots$O pseudospins and the molecular ions PO_4^{3+} and NH_4^+ of the lattice distinguishes between electric dipole glass and magnetic spin glass. Therefore temperature dependence of PO_4 and NH_4 molecular vibrations may well be informative of the freezing dynamics in the dipole glass system. Raman scattering sensitive to the site symmetries of the concerned molecules can give this information of glass transition by temperature dependent changes of Raman bands. Raman scattering studies of many dipole glass systems have been made in $Rb_{1-x}(NH_4)_xH_2PO_4$ (RADP-x) mixed crystal,[4–7] $K_{1-x}(NH_4)_xH_2PO_4$ (KADP-x),[8] $Rb_{1-x}(ND_4)_xD_2PO_4$ (DRADP-x)[9,10] and $Rb_{1-x}(ND_4)_xD_2AsO_4$ (DRADA-x) systems.[11]

In the present work of ours we want to report our results of Raman-scattering studies on $Cs_{1-x}(NH_4)_xH_2AsO_4$ (CADA-x) mixed crystals, the dipole glass phase diagram of which was reported very recently.[12]

II. EXPERIMENT

Powders of CsH_2AsO_4 (CDA) and $NH_4H_2AsO_4$ (ADA) are obtained from the saturated solutions of cesium carbonate and arsenic acid in appropriate molar concentration, and also between ammonium carbonate and arsenic acid, respectively. From these powders of CDA and ADA we can obtain the saturated solutions of CADA-x to grow single crystals by the slow cooling method. Mixing concentration x of the grown CADA-x crystals was determined by the atomic absorption chemical analysis. The Raman sample was cut to the size of $1.0\times6.0\times5.5$ mm^3. Raman scattering excitation was made by use of the Ar ion laser operated at $\lambda = 488.0$ nm and output power of 200 mW.

Double grating monochrometer (Jobin Yvon-U 1000), thermoelectrically cooled PM tube, and 90° scattering geometry were used to detect Raman signals. Low temperature measurements were made by use of the closed cycle He refrigerator (Displex, APD Ltd.) with temperature controller (Lake Shore-DRC91CA) employing silicon diode sensors. The temperature stability was better than ± 0.1 K with the local temperature at the scattering volume determined from the Boltzmann statistics of Stokes and anti-Stokes Raman intensities. There was a deviation as large as 10 K from the apparent sensor reading of local temperature.

III. RESULTS AND DISCUSSION

Factor group analysis of KDP-type crystals undergoing the structural phase transition from tetragonal (D_{2d}) to orthorhombic (C_{2v}) lattice has been well known but with debates on the site symmetry assignments for PO_4 and NH_4 tetrahedra still remaining. The factor group analysis of KDP-type crystal[11,13] gives $\Gamma_{vib}=4A_1+5A_2+6B_1+6B_2+12E$, where A_1, B_1, B_2, and E species are all Raman active. The site symmetry of the AsO_4 tetrahedron was determined on the basis of the correlation tables for the internal modes as S_4 or C_2.[14,15] According to this anlysis all the internal modes of AsO_4 from ν_1 to ν_4 are Raman active in the A_1 species.[13–15]

Simon[13] assigned the site symmetry change from S_4 to C_2 across the ferroelectric transition of the KDP family crystals but from S_4 to C_1 across the antiferrolelectirc transition of the ammonium dihydrogen phosphate (ADP)-type crystals. Tominaga,[14] however, assigned C_2 site symmetry for KDP crystal in both paraelectric and ferroelectric phases with the S_4 site symmetry in the paraelectric phase only possible as a

 ©1999 The American Physical Society

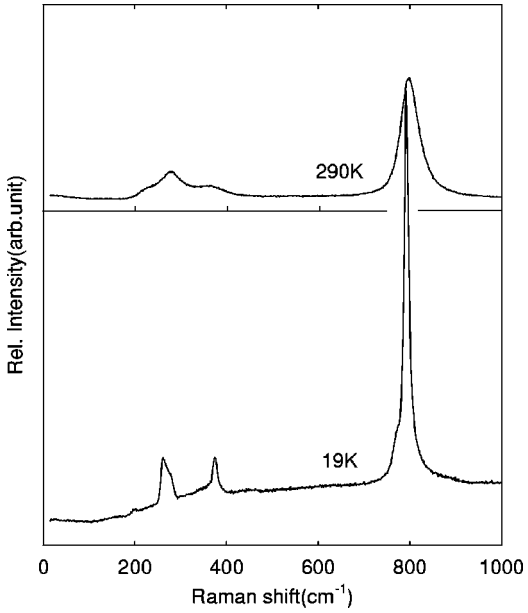

FIG. 1. Raman spectra observed at $T=290$ K and 19 K in the scattering geometry of $x(zz)y$ selecting A_1 modes.

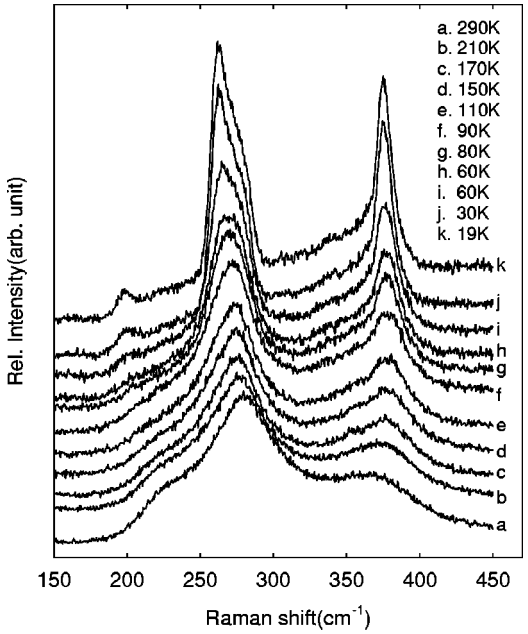

FIG. 2. A_1-symmetry Raman bands derived from the doubly degenerated ν_2 and triply degenerated ν_4 bending modes of AsO_4 observed in the $x(zz)y$ configuration as a function of temperature.

random average. Kasahara and co-workers[15,16] also assigned C_2 site symmetry in the paraelectric phase but C_1 site symmetry in the antiferroelectric phase of ADP-type crystals.

In the mixed CADA-x ($x=0.20$) crystal NH_4^+ ions, randomly substituting Cs^+ ions, should give rise to random bias fields to the O-H$\cdots$O bonds through the extra hydrogen bonding of N-H$\cdots$O and thus lead to distortions of both NH_4 and AsO_4 tetrahedra. As a result the site symmetry of both NH_4 and AsO_4 tetrahedra in the mixed crystal may be lowered to C_2 already at room temperature as compared with the respective parent crystals. Although CADA-x ($x=0.20$) crystal was found to undergo the transition from paraelectric to dipole glass phase by dielectric measurements,[12] we have no experimental data available to confirm the dipole glass transitions for other extended x values of CADA-x single crystal. It is very difficult to grow the CADA-x crystals of good optical quality because of the large difference in ionic size between Cs^+ and NH_4^+.

In Fig. 1 we have shown Raman spectra of A_1-symmetry modes observed at $T\simeq 290$ and 19 K. More details of the spectra in the region of 150–450 cm^{-1} are shown in Fig. 2 as observed at various temperatures, where we can assign the Raman bands at around 280 and 350 cm^{-1} as derived from a doubly degenerate bending mode ν_2 and a triply degenerate bending mode ν_4 of AsO_4 internal vibrations, respectively. In Fig. 3 we tried to fit the complex Raman spectra of ν_2 and ν_4 modes in terms of four Lorentzian bands in the range of temperature 290–90 K but below 90 K another new band started to appear, which required an additional Lorentzian band at 280 cm^{-1} for better fitting. This additional band may represent a splitting of the doubly degenerate ν_2 bending mode.

Although a splitting of both ν_1 mode (A_1 symmetry) and ν_4 mode (E symmetry) was reported at low-temperature spectra of DRADP-x crystal,[9,10] we have no previous reports of splitting in the A_1 symmetry internal modes in other dipole glass systems. The very large ionic size of Cs^+ in CADA-x crystal may cause a larger local strain in the mixed crystal so that the degenerated internal modes of AsO_4 may have been split. Ionic sizes of NH_4^+, Rb^+, and Cs^+ are known to be 1.42, 1.48, and 1.67 Å, respectively.[2]

In Fig. 4 we have shown the temperature dependence of the Raman spectra in the region of 700–900 cm^{-1}, which

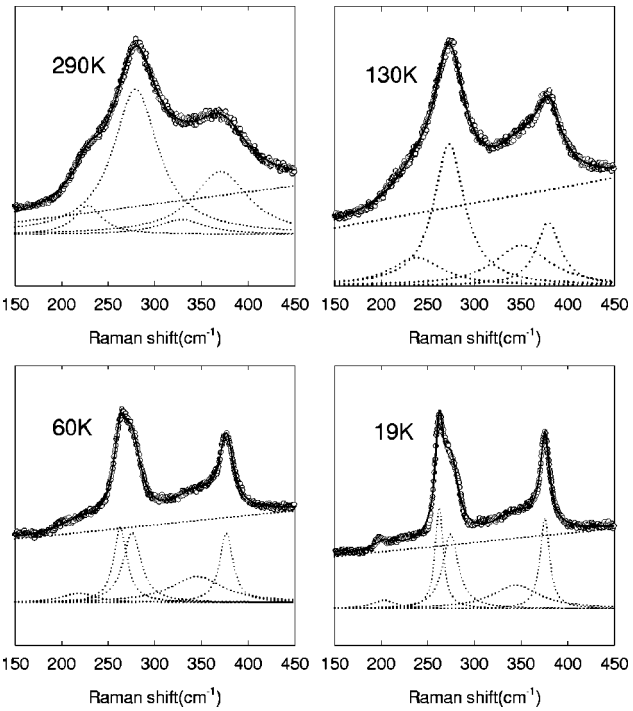

FIG. 3. Best-fit analysis of temperature dependence of Raman band profiles in terms of Lorentzian component bands for selected Raman bands from Fig. 2: dotted lines represent Lorentzian components, solid lines the best-fit profiles, and open circles the experimental observations.

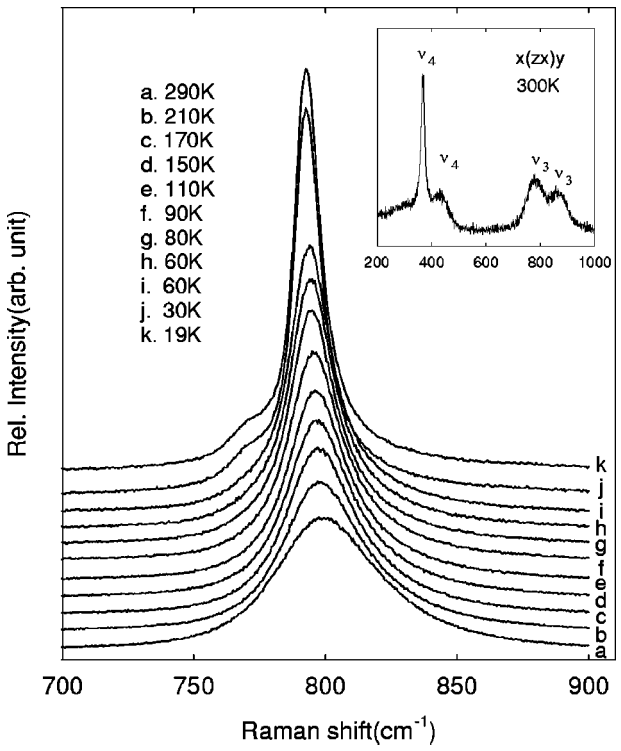

FIG. 4. A_1-symmetry $x(zz)y$ Raman spectra in the region showing the symmetric stretching ν_1 mode and asymmetric stretching ν_3 mode of AsO_4 observed as a function of temperature. In the inset $x(zx)y$-E mode Raman bands are shown, where ν_3 and ν_4 internal modes of AsO_4 are selected.

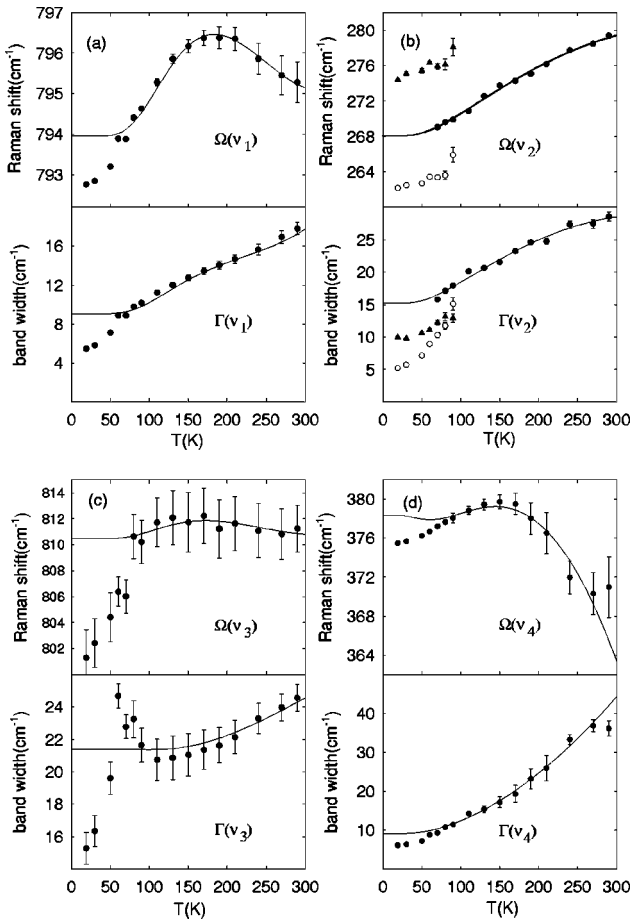

FIG. 5. Frequency and bandwidth dependence on temperature for the ν_1, ν_2, ν_3, ν_4 internal modes of AsO_4 belonging to the A_1 symmetry of $x(zz)y$ scattering configuration. The solid lines represent the normal temperature dependence expected from the third and fourth anharmonic interactions.

are derived from symmetric stretching ν_1 mode and antisymmetric stretching ν_3 mode. If we assign the site symmetry of AsO_4 in the paraelectric phase as C_2 all internal modes of AsO_4 should be allowed in the A_1 symmetry Raman spectra.[14,15] We thus expect to observe two internal modes of AsO_4 in the frequency region of Fig. 4. In the inset of Fig. 4 we have depicted E-symmetry Raman bands observed at room temperature, where we expect only ν_3 and ν_4 modes. The E-mode bands between 750 and 950 cm^{-1} may thus be assigned to ν_3 modes. With the mode assignments given to each band we have applied the best-fit analysis to the spectra in terms of Lorentzian component bands. The best-fit results of peak positions and bandwidths of the corresponding Lorentzian components are shown in Figs. 5(a)–5(d).

Wesselinowa, Apostolov, and Filipova[17] incorporated harmonic phonon excitations, anharmonic phonon-phonon interactions and spin-phonon interactions to the pseudospin Ising model. From the Green's function calculation of renormalized phonon energy they found the temperature dependence of phonon energy at temperatures above phase transition in the pseudospin Ising model systems as coming from the third and fourth order anharmonic phonon-phonon interactions.

Since we expect a greater anharmonic effect in the glass forming system we may adopt this effect of the anharmonicity to fit the temperature dependence of the observed peak frequency and bandwidth. In terms of the third and fourth anharmonic interaction constants we can write for the temperature dependence of frequency $\Omega_j(T)$ and damping constants $\Gamma_j(T)$ of the jth phonon as[18–20]

$$\Gamma_j(T)=\gamma_{0j}+A\left(1+\frac{2}{e^x-1}\right)+B\left(1+\frac{3}{e^y-1}+\frac{3}{(e^y-1)^2}\right), \tag{1}$$

$$\Omega_j(T)=\omega_{0j}+C\left(1+\frac{2}{e^x-1}\right)+D\left(1+\frac{3}{e^y-1}+\frac{3}{(e^y-1)^2}\right), \tag{2}$$

where $x=\hbar\omega_{0j}/2kT$, $y=\hbar\omega_{0j}/3kT$, ω_{0j} represents harmonic frequency of mode j, and γ_{0j} broadening as due to static defects and imperfections. The parameters A, B, C, and D represent the third- and fourth-order anharmonic constants of the Klemens' approximation,[21] where assumption is made as $\omega_1=\omega_2=\omega_o/2$ and $\omega_1=\omega_2=\omega_3=\omega_o/3$ in the anharmonic phonon interactions of the third and fourth orders, respectively.

In Fig. 5 the solid lines represent the theoretical fits of Eqs. (1) and (2) with best-fit parameters given in Table I. From the table we can see the symmetric stretching mode (ν_1) is most susceptible to the third order (A, C) and fourth order (B, D) anharmonic interactions, and for all the internal modes the third order anharmonicity (A, C) is far greater than the fourth order anharmonicity (B, D), and the zero-temperature effective anharmonicity $\gamma(0)$ is greatest for the

TABLE I. Best-fit values of harmonic frequencies and anharmonic parameters: $\gamma(0)=\gamma_0+A+B$.

	$\omega_0(\mathrm{cm}^{-1})$	A	B	$\lvert B/A\rvert$	$\gamma(0)(\mathrm{cm}^{-1})$	C	D	$\lvert D/C\rvert$
ν_1	913.1	−164.3	42.41	0.25	9.05	−152.7	33.54	0.22
ν_2	258.7	13.76	−1.09	0.08	15.26	10.05	−0.70	0.07
ν_3	882.2	24.09	−2.69	0.11	21.40	−91.66	19.66	0.22
ν_4	346.9	2.87	3.24	1.13	9.12	39.40	−7.97	0.20

asymmetric stretching mode (ν_3). The fit can be seen to fail completely from below $T\simeq 80$ K. This observation conforms with the previous reports on the x-ray diffraction results of RADP-x crystals[22,23] that the lattice constants and thus the unit-cell volume start to deviate from the classical anharmonicity temperature dependence at a well defined temperature, where short range ordering is developed to enhance the mean square local polarizations and thus electrostrictive coupling. The increasing lattice constants are expected to decrease the vibrational frequencies but local ordering should reduce the bandwidth.

In Fig. 6 we have shown the low-frequency Raman spectra of B_2-symmetry modes, where we can observe the Cs-AsO_4 translatory mode coupled with a collective proton mode, and also a separate NH_4-AsO_4 translatory mode. The NH_4-AsO_4 translatory mode favors for the lateral Slater configurations of protons and may not be coupled with the same collective proton mode of up-down Slater configurations. The solid lines represent the best fit curves in terms of coupled harmonic oscillators. The response function and thus the Raman susceptibility χ'' of the coupled system are obtained from[4]

$$\begin{pmatrix} \omega_1^2-\omega^2-i\omega\gamma_1 & -i\omega\gamma_{12} & 0 \\ -i\omega\gamma_{12} & \omega_2^2-\omega^2-i\omega\gamma_2 & 0 \\ 0 & 0 & \omega_3^2-\omega^2-i\omega\gamma_3 \end{pmatrix} \times \begin{pmatrix} G_{11} & G_{12} & G_{13} \\ G_{21} & G_{22} & G_{23} \\ G_{31} & G_{32} & G_{33} \end{pmatrix} = \begin{pmatrix} 1 & 0 & 0 \\ 0 & 1 & 0 \\ 0 & 0 & 1 \end{pmatrix},$$

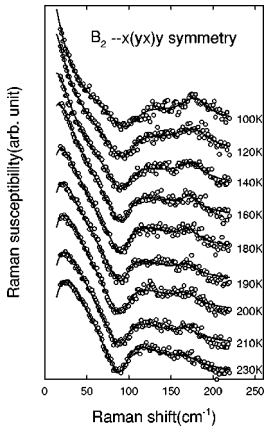

FIG. 6. Raman susceptibility profiles derived from the low-frequency Raman spectra of B_2-$x(yx)y$ symmetry external modes observed at various temperatures. The solid lines represent the best fits in terms of two coupled harmonic oscillators and another additional harmonic oscillator band.

$$\chi''(\omega)=\sum_{i,j} P_i P_j G_{ij}(\omega),$$

where $P_{i,j}$ represents the respective mode strength of the three harmonic oscillator modes ω_1, ω_2, and ω_3. Raman scattering Stokes intensity is then obtained by

$$I(\omega)=[n(\omega)+1]\chi''(\omega),$$

where $n(\omega)$ is the Bose-Einstein factor of phonon thermal population at ω.

In Fig. 7 the temperature dependence of the best fit parameters in the coupled oscillator model are shown as obtained. As can be seen in Fig. 7(b) ω^2/γ was obtained to best fit the soft-mode temperature dependence of $a(T\text{-}T_o)$ with $T_o\simeq 28.8$ K. The standard error bar of the fitting increases steeply at temperatures below 100 K and we did not include our results of the fit. The abrupt change may originate from the growing intensity of the AsO_4 libration band in the same region between 100 and 200 cm^{-1}, the increasing selection rule violations due to the random fields of NH_4^+, and the

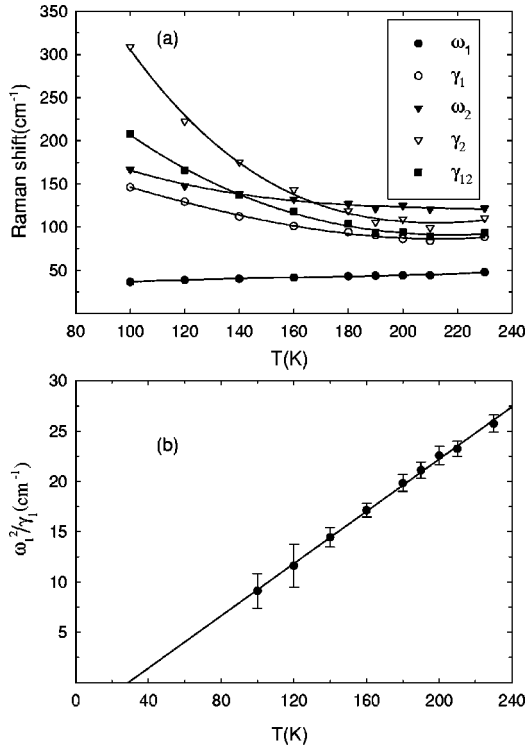

FIG. 7. Temperature dependence of the best-fit parameters for low frequency B_2-symmetry bands as obtained from the coupled harmonic oscillator band analysis of Fig. 6: (a) ω_1, γ_1, ω_2, γ_2, and γ_{12}, the solid lines are simply for guiding eyes. (b) ω_1^2/γ_1, the solid line represents the best fit for $\omega_1^2/\gamma_1=a(T\text{-}T_o)$.

simplified coupled mode analysis fails to describe the complex spectrum in this region.[4] However, the temperature dependence of Fig. 7 for the harmonic oscillator soft-mode may well be extended to below 100 K if we could assume all these subsidiary effects of the ensuing additional bands were not coupled with the soft mode. It is interesting to observe the resonance type soft mode of $\omega_1^2 = a(T\text{-}T_o)$ in KDA, RDA, and CDA ferroelectric crystals[24,25] but the relaxation-type soft mode in dipole glass systems such as RADP-x and RADA-x mixed crystals.[4,7] In general it is believed that the proton tunneling system gives rise to the resonance type soft mode while the relaxation type soft mode is expected in the double-well pseudospin system when tunneling is absent.[26]

In the RADP-x dipole glass system it has been found from NMR experimental results[27] that thermally activated hopping is a dominant process at temperatures above $T \simeq 25$ K, and we expect a critical slowing down of the relaxation time since in the double-well potential of protons thermal hopping prevails rather than quantum tunneling in the dipole glass. The observation of $T_o \simeq 28.8$ K for the relaxational soft-mode condensation in our system of CADA-x ($x = 0.20$) is at a large deviation from the freezing onset temperature of $T_f \simeq 80$ K where the internal modes of molecular vibration start to show anomalies. This large deviation between the two temperatures was also obtained in both RADP-x and RADA-x crystals as large as 65 and 55 K, respectively.[4,7,28]

The extrapolated condensation temperature of the resonance-type optical soft mode in the ferroelectric RDA crystal[25] was observed to be much lower than the structural phase transition temperature, which was attributed to the repulsive anticrossing piezoelectric coupling between the optical soft mode and the acoustic mode. The internal vibrations of molecules should be affected mostly by the structural transition driven by the acoustic soft mode involving anisotropic changes in lattice constants and thus site symmetries.

In dipole glass we expect large local electrostrictions due to randomly freezing short range orders in addition to the piezoelectirc strains. Piezoelectric and electrostrictive effects are additive to give an effective piezoelectric constant[29] h_{eff} of $(h_{\text{eff}})^2 \simeq h^2 + 4R^2 q_{\text{EA}}$, where h is piezoelectric coefficient, R electrostrictive coefficient, and q_{EA} Edward-Anderson type order parameter. This enhanced effective piezoelectric constant leads to the enhanced repulsive anticrossing gap between the soft-mode optic phonon and the xy shear mode acoustic phonon so that a greater temperature gap will be effected between the extrapolated condensation temperature of the soft-mode optic phonon and the coupled acoustic soft mode.

Thus the molecular vibrational bands sensitive to the structural deformations should follow the temperature dependence of the coupled acoustic soft mode whose condensation temperature is well above the extrapolated condensation temperature of the soft-mode optic phonon as in the piezoelectric ferroelectric crystals.

IV. CONCLUSION

In the CADA-x ($x = 0.20$) mixed-crystal temperature dependence of Raman scattering spectra was studied in detail. A_1 symmetry molecular vibrational bands of AsO_4 are found to deviate strongly from the normal temperature dependence of the third and fourth order anharmonic phonon-phonon interactions at temperatures below $T_f \simeq 80$ K. This anomalous temperature dependence below T_f is attributed to the onset of short-range ordering of protons, which enhances local cluster polarizations and thus electrostrictive local strains.

B_2 symmetry optic soft mode was analyzed in terms of temperature dependent harmonic oscillator coupled modes. The satisfactory best fit was possible only for ω^2/γ (inverse relaxation time), which tends to zero at $T_o \simeq 28.8$ K.

This observation of the relaxational type soft mode also implicates that the thermally activated hopping should be a more significant process than quantum tunneling in this CADA-x pseudospin double well random system at least in the temperature region of our Raman spectroscopic observation.

*Author to whom correspondence should be addressed.

[1] E. Courtens, J. Phys. (France) Lett. **43**, L199 (1982).
[2] E. Courtens, Ferroelectrics **72**, 229 (1987).
[3] U. T. Höchli, K. Knorr, and A. Loidl, Adv. Phys. **39**, 405 (1990).
[4] E. Courtens and H. Vogt, J. Chim. Phys. Phys.-Chim. Biol. **82**, 317 (1985).
[5] E. Courtens and H. Vogt, Z. Phys. B **62**, 143 (1986).
[6] T. Hattori, H. Araki, S. Nakashima, A. Mitsuishi, and H. Terauchi, J. Phys. Soc. Jpn. **56**, 781 (1987); **57**, 1127 (1988).
[7] J.-J. Kim and H.-K. Shin, Ferroelectrics **135**, 319 (1992).
[8] J.-J. Kim and W. F. Sherman, Phys. Rev. B **36**, 5651 (1987).
[9] Y. I. Yuzyuk, I. Gregora, V. Vorlíček, J. Pokorný, and J. Petzelt, J. Phys.: Condens. Matter **7**, 683 (1995).
[10] Y. I. Yuzyuk, I. Gregora, V. Vorlíček, and J. Petzelt, J. Phys.: Condens. Matter **8**, 619 (1996).
[11] C.-S. Tu, R.-M. Chien, and V. H. Schmidt, Phys. Rev. B **55**, 2920 (1997).
[12] T. K. Song, S. E. Moon, K. H. Noh, S.-I. Kwun, H. K. Shin, and J.-J. Kim, Phys. Rev. B **50**, 6637 (1994).
[13] P. Simon, Ferroelectrics **135**, 169 (1992).
[14] Y. Tominaga, Solid State Commun. **49**, 153 (1983).
[15] M. Kasahara, M. Tokunaga, and I. Tatsuzaki, J. Phys. Soc. Jpn. **55**, 367 (1986).
[16] Y. Hayashi, M. Kasahara, M. Tokunaga, and I. Tatsuzaki, J. Phys. Soc. Jpn. **57**, 1321 (1988).
[17] J. M. Wesselinowa, A. T. Apostolov, and A. Filipova, Phys. Rev. B **50**, 5899 (1994); Phys. Status Solidi B **197**, 509 (1996).
[18] M. Balkanski, R. F. Wallis, and E. Haro, Phys. Rev. B **28**, 1928 (1983).
[19] K. C. Serra, F. E. A. Melo, F. M. Filho, J. E. Moreira, and V. Lemos, Phys. Status Solidi B **170**, 113 (1992).
[20] B. Berthevile, H. Bill, and H. Hagemann, J. Phys.: Condens. Matter **10**, 2155 (1998).
[21] P. G. Klemens, Phys. Rev. **148**, 845 (1966).
[22] E. Courtens, T. F. Rosenbaum, S. E. Nagler, and P. M. Horn, Phys. Rev. B **29**, 515 (1984).

[23] H. Terauchi, T. Futamura, Y. Nishinata, and S. Iida, J. Phys. Soc. Jpn. **53**, 483 (1984).
[24] R. P. Lowndes, N. E. Tornberg, and R. C. Leung, Phys. Rev. B **10**, 911 (1974).
[25] M. A. Pimenta, J. M. Filho, M. S. Dantas, F. E. A. Melo, and A. S. Chaves, Phys. Rev. B **57**, 22 (1998).
[26] R. Blinc and B. Žekš, *Soft Modes in Ferroelectrics and Antiferroelectrics* (North-Holland, Amsterdam, 1974).
[27] J. Dolinšek, D. Arčon, B. Zalar, R. Pirc, R. Blinc, and R. Kind, Phys. Rev. B **54**, 6811 (1996).
[28] H. K. Shin and J.-J. Kim, Ferroelectrics **125**, 443 (1992).
[29] E. Courtens, R. Vacher, and Y. Dagorn, Phys. Rev. B **33**, 7625 (1986).